中國機械工程學刊第四十卷第二期第 161~170 頁(民國一百零八年)
Journal of the Chinese Society of Mechanical Engineers, Vol.40, No.2, pp 161~170 (2019)

# Novel Range Image Segmentation Using Region-Growing and Surface Classification

Liang-Chia Chen[*], Ching-Wen Liang[***], Xuan-Loc Nguyen[***] and Shyh-Tsong Lin[**]

**Keywords**: Automated optical inspection (AOI), 3-D measurement, 3-D object segmentation, range image, region growing.

## ABSTRACT

In the article, a novel method for object segmentation using surface characteristics of range images is presented to solve the problem of digital background identification (DBI) in 3-D measurement. The proposed method uses a novel criterion based on the distribution of normal surface vectors for 3-D surface (or object) segmentation. According to this criterion, scanned range data from measured objects is first classified into several types of surface as an initial stage of evaluation for addressing all the measured points belonging to the imaging background. By incorporating this criterion into the region-growing process, a robust range-data segmentation algorithm capable of segmenting complex objects, which may be suffered with huge amount of noises from a real field condition, is established. Furthermore, to detect the object boundary accurately, a recursive search process involving the region-growing algorithm for registering homogeneous surface regions is developed. Experiments from several scenarios using a laser 3-D scanner demonstrate the feasibility and effectiveness of the proposed method for 3-D object segmentation and localization in automated optical inspection (AOI).

## INTRODUCTION

One of the most important issues in 3-D imaging is to develop an effective object segmentation (OS) algorithm for object localization or recognition, especially for automated optical inspection (AOI). The main task involved in object segmentation is to precisely classify scanned point clouds into the foreground and the background.

*Paper Received May, 2017. Revised October, 2017. Accepted November, 2017. Author for Correspondence: Liang-Chia Chen*

[*] *Professor, Department of Mechanical Engineering, National Taiwan University and Institute of Automation Technology, National Taipei University of Technology, Taipei, Taiwan, 10617, R.O.C. lchen@ntu.edu.tw*

[**] *Professor, Department of Electro-Optical Engineering, National Taipei University of Technology, Taipei, Taiwan, 10608, R.O.C.*

[***] *Graduate Student, Institute of Automation Technology, National Taipei University of Technology, Taipei, Taiwan, 10608, R.O.C.*

Contrary to providing better segmentation results, OS using range images involves more work than traditional 2-D image segmentation methods due to the complexity of data. The foreground is often highly entangled and sometimes mixed with the background because the data acquired from various sensing devices are usually noisy with a low signal-to-noise (S/N) ratio.

With many powerful light detection and ranging (LIDAR) devices available in the market, the acquisition of 3-D range data becomes more feasible and popular. These devices can capture high-resolution data of objects, such as people, cars, trees, buildings and roads. Along with such trend, related techniques and strategies have been proposed in the literature. Previous studies on range image segmentation were inspired by the traditional 2-D image processing techniques in object contour and morphological operators since 2-D image methods are available and have been well studied (Jiang et al., 1999, 2000). Region-based and edge-based techniques are two important directions in range image segmentation research. Region-based segmentation algorithms involve detecting continuous surfaces with similar geometrical properties; hence, the method is stable for marking object regions (Bogoslavskyi, 2016; Gharavi, 2007; Golovinskiy, 2009; Holz, 2012; Muller et al., 2002). The main drawback of this technique is that it is not very accurate in marking the object boundary and may produce distorted results. In comparison, edge-based techniques can provide more accurate results in determining object boundary, but they have problems defining objects from the detected edges. One of the edge-based techniques proposed is a binary edge map that allows quick processing of very large range images (Sappa, 2001, 2006). With a binary edge map generated, a contour detection strategy is developed for extracting different boundaries. On the other hand, the region-based technique detects continuous surfaces by classifying individual objects according to their geometrical properties (Chen et al., 2010; Lee et al., 1998). In an initial study, normal surface vectors have been employed to define surface continuity according to homogeneity criteria (Pulli, 1992). Moreover, some other methods can detect surface discontinuities if the object contours can be easily segmented (Silva et al., 2001; Stiene et al., 2006). In other studies, the information provided by the edge detection process is taken as a clue for estimating the number of regions required to initialize the clustering algorithm, which can be called the hybrid technique (combining edge-based and region-based) (Koster, 2000). Some researches define the slope value of a point to its neighbors as a criterion for separating the background and foreground (Roggero, 2001; Sithole, 2001). These methods have similar ideas with morphological operators, in which the window size that defines a neighboring region has to be chosen carefully in order to deal with data having variation in surface roughness. Another clustering method groups point clouds into various clusters according to point distances (Klasing et al., 2008). To include more information for object segmentation, the gray-scale image was included to perform more robust OS (Chang et al., 2008; Heisele et al., 1999; Neira et al., 1999). In this case, both depth and gray-scale information are acquired simultaneously using the same optical scanner, in which the gray-scale image provides contextual information for determining the object's location. Furthermore, to connect a 3-D point with its neighboring region for forming an object, the k-nearest neighbor graph method can perform foreground and background segmentation by presetting a background prior and foreground constraints for defining a min-cut index (Golovinskiy et al., 2009).

The proposed method uses region-growing techniques that retrieve objects according to their homogeneous property. The region-growing process is guided by regional feature analysis to cluster data into several groups, in which no parameter tuning or a priori knowledge is required (Chang et al., 1994). In this paper, we present our recent efforts in developing segmentation algorithms for human perception, where objects segmented are texture-consistent regions. The originality of this work lies in the fact that segmentation is performed in a novel two-stage process. The background is first identified and the objects underlying detection are then segmented using the proposed criteria in the region-growing process. The proposed algorithm can accurately mark the boundary of the segmented object, thus overcoming the existing major problem encountered in region-growing methods.

Meanwhile, a novel method for digital background identification (DBI) is proposed by exploring the uniformity of normal vector distribution to identify the seeds for growing the background region. One of the difficulties for general OS techniques is that the background can lie in various locations or has been split into a random number of pieces, which may be further segmented undesirably as objects. Although DBI has attracted much research interest (Evans et al., 2007; Lu et al., 2009), it remains one of the most challenging tasks in OS. The key problem is that since the selection of seeds may significantly influence the accuracy of final segmentation, OS may be forced to follow a semi-automatic approach that requires human intervention (Sithole et al., 2004), which would become a major drawback for any practical application. To overcome this disadvantage, the proposed approach combines an initial process of classifying surface types with performing least-squares plane fitting (so-called scene ground detection) for determining initial seeds of the background. Our experimental results show that the proposed method is capable of segmenting multiple objects within a detection range of up to a few hundred meters with detecting targets in various arrangements. The developed method is proven superior to traditional clustering and region-growing methods.

The rest of the paper is organized as follows. The segmentation algorithm is presented in the next section with the introduction of surface characteristics and the plane-fitting process for detecting the background. Section 3 describes the experimental design and analyzes OS results obtained from detecting some real scenes. Section 4 concludes the paper.

## METHODOLOGY

The developed method begins with classifying point clouds in range images into three different surface types, namely uniform, rough and noisy surfaces, according to the distribution of the normal surface vectors. Following this, the scene ground is then detected by applying least-squares plane fitting to the surface region being classified as a uniform surface. Furthermore, to localize accurately the scene ground, a region-growing process is developed to extend the homogeneous region of an object region initially segmented in the first stage. As a result, all the individual objects existing in range images can be segmented using a recursive search algorithm after the scene ground is removed. Figure 1 summarizes the series of steps involved in the proposed method.

### Surface classification for DBI

Surface classification is an important step in the initial detection of the ground, objects and edges between different surface regions. It involves calculating first the surface normal vector from a 3-D point with its neighboring region and then classifying the point clouds into three different surface types. The classification process of point clouds is illustrated in Figure 2. The Class I, Class II and Class III are uniform, rough and noisy surfaces type respectively.

Before calculating the normal vectors, noises are first removed by a median filter since the range data may contain many dropouts and outliers. The position and orientation of the tangent plane of each point in a 3-D model also need to be determined, as shown in Figure 3. The orientation of a tangent plane shows the direction of the normal vector at that point. Since the point cloud data are unorganized, when determining the orientation, the neighboring planes must be consistently oriented, meaning that the orientations of neighboring points have to be similar.

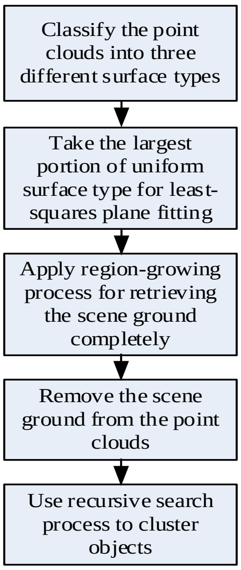


Figure 1. Flow chart of the proposed method.

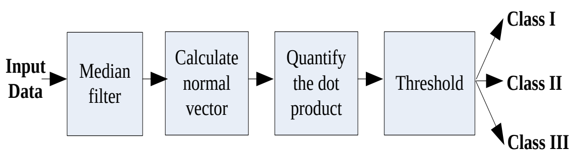


Figure 2. Classification process of point clouds into three surface types.

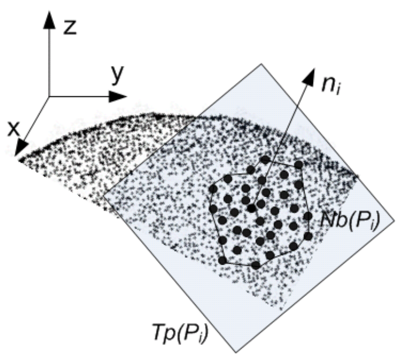


Figure 3. Construction of a tangent plane on a 3-D model.

Here, we define the tangent plane $Tp(P_i)$ of a point $P_i$ in the point clouds. The center point and normal vector for $Tp(P_i)$ are determined by gathering the group of points denoted by $Nb(P_i)$, which is called the neighborhood of $P_i$. The center point $O_i$ is taken to be the centroid of $Nb(P_i)$ and the normal vector $\vec{n}_i$ is determined using the *principal component analysis* (PCA). The proposed method calculates the normal vector $\vec{n}_i$ by forming the covariance matrix of $Nb(P_i)$. The covariance matrix is a symmetric 3 x 3 and positive-definite matrix whose all the eigenvalues are positive real as follows:

$$CV_i = \sum_{P \in Nb(P_i)} (P - O_i) \otimes (P - O_i) \qquad (1)$$

where $\otimes$ denotes the outer product vector operator.

The eigenvalues of $CV_i$ are then calculated as $\lambda_i^1 \geq \lambda_i^2 \geq \lambda_i^3$, which correspond to the three unit eigenvectors $v_i^1 \geq v_i^2 \geq v_i^3$, respectively. The normal vector $\vec{n}_i$ is chosen to be either $v_i^3$ or $-v_i^3$, depending on the orientation of its neighboring normal vectors.

The dot product of two vectors can represent the tilting angle between them. As seen in Figure 4(a), the average dot product between the normal vector of the point underlying evaluation and its neighboring points is taken as a surface index for initial surface type classification. Examples of a uniform surface region and a surface edge are shown in Figure 4(b) and (c), respectively. As can be seen, the distribution of the normal vectors in a uniform surface has in general higher uniformity than that along a surface edge region. Accordingly, the point clouds can be initially classified into three different surface types for further processing. The average dot product is calculated as follows:

$$\bar{\delta} = \frac{1}{m}\left(\sum_{All\ neighbour\ points\ (i=\overline{1,m})} \delta_i\right) \qquad (2)$$

where $m$ is the number of neighboring points; and $\delta_i = \frac{\vec{n} \cdot \vec{n}_i}{|\vec{n}||\vec{n}_i|}$ is the mean dot product between the normal vector of the point $\vec{n}$ and the normal vector of its $i^{th}$ neighboring point $\vec{n}_i$.

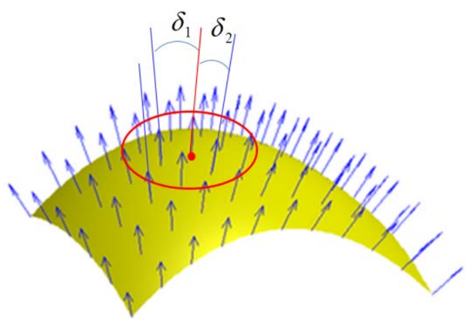


(a)

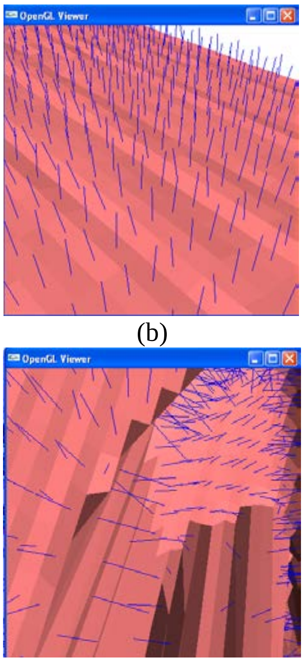

(b)

(c)

Figure 4. Surface type classification by judging the distribution of normal vectors: (a) illustration of dot products between the normal vector of the inspecting point and those of its neighbors; (b) example of a uniform surface type; and (c) example of an edge surface type.

In the proposed method, three surface types are determined by the distribution of the mean dot product and are classified into uniform (green), rough (red) and noisy surfaces (blue), as shown in Figure 5. Since the dot products belong to [0, 1], two present thresholds, $\Delta_1$ and $\Delta_2$, are employed to classify the surface type, where $0 \leq \Delta_2 < \Delta_1 \leq 1$. According to the noise level of range data obtained from a specific sensing device, $\Delta_1$ and $\Delta_2$ can be adequately preset to best segment the point clouds. $\Delta_1$ and $\Delta_2$ are set to be 0.9 and 0.4, respectively, to suit the 3-D range scanner employed in this research.

After surface classification, the point cloud U is split into several local regions with different surface types: $U = \{U_1, U_2, .., U_M\}$ where M is the number of classified regions. The scene ground in range image is retrieved by performing least-squares plane fitting to the largest uniform surface region within the scene. Since the scene ground generally lies on a more uniform surface region, the uniform surface is taken as the part of the scene ground. Furthermore, since the scene ground usually occupies the largest uniform surface area in the scene, the cardinality of a set $U_i$, denoted $\overline{\overline{U_i}}$, is used as a factor to detect the uniform region for least-squares plane fitting.

$$U_{fitting} = \left\{ U_k \middle| \begin{array}{c} U_k \in \mathrm{U}, \bar{\delta}(U_k) \geq \Delta_1, \\ \overline{\overline{U_k}} = \max\{\overline{\overline{U_i}} \,|\, U_i \in U, \bar{\delta}(U_i) \geq \Delta_1\} \end{array} \right\} \quad (3)$$

Plane fitting is employed to determine the best plane fitted with selected point clouds. The process is performed using least-squares approximations for $U_{fitting}$. After the parameters of the fitting plane are calculated, a group of points $U_{Seed}$ which satisfy the condition of elevation restriction are taken as the seeds in the region-growing process for retrieving the scene ground. The following constraint is employed to determine the seeds for the region-growing process:

$$U_{Seed} = \{\mathrm{p(x,y,z)} | \mathrm{p} \in \mathrm{U}, |Ax + By + Cz + D| < \varepsilon\} \quad (4)$$

where $\varepsilon$ is a positive number; *A*, *B*, *C* and *D* are the fitting coefficients which satisfy the optimal condition of the least squares method.

Figure 5 shows an example of generating seeds for the subsequent growing process. First, surface classification was applied to the 3-D range image (Figure 5(b)), followed by least-squares plane fitting to the largest uniform surface region (Figure 5(c)), and finally the points that satisfy the fitting condition can be retrieved (Figure 5(d)).

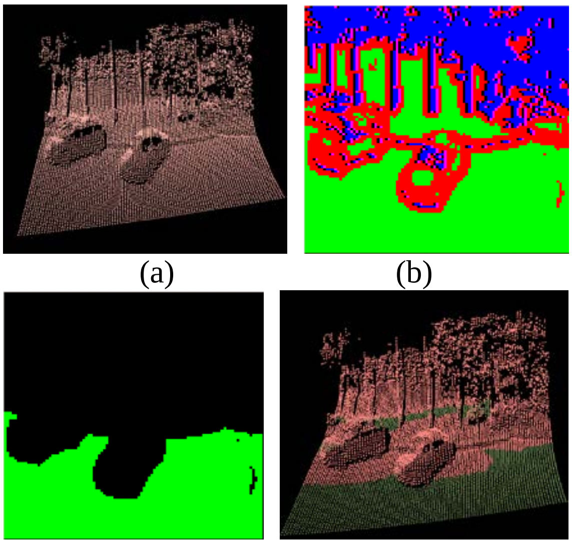

(a) (b)

(c) (d)

Uniform surface (point property $\bar{\delta} \geq \Delta_1$)

Rough surface (point property $\bar{\delta} > \Delta_2$ and $\bar{\delta} < \Delta_1$)

Noisy surface (point property $\bar{\delta} \leq \Delta_2$)

Figure 5. Classification of surface regions: (a) a 3-D range image; (b) classification of surface types; (c) the largest portion of uniform surface and (d) the points that satisfy the condition of plane fitting.

**Region-growing Algorithm for DBI**

The idea of using region-growing algorithm in OS is to grow distinct image regions represented by some pixels (seeds) until none of the neighboring pixels satisfy the growing condition. In the proposed method, the background is completely retrieved according to those seeds found by plane fitting. A rule defined for region-growing is to describe a growth mechanism and to check the homogeneity of the region after each growth step. At each stage N for the background G, the method evaluates whether there are unclassified points existing in the neighborhood of the region border. When N = 0, G = $U_{Seed}$ , N is further increased and a point x is assigned to the background G to examine if the region homogeneity, P(G) = TRUE, is valid. The growing process continues if the condition is satisfied. Otherwise, the growing process will be suspended.

The arithmetic mean m and standard deviation σ of a class $R_i$ having n points:

$$m = \frac{1}{n} \sum_{p(x,y,z)\epsilon R(i)} d(p(x,y,z),\alpha) \qquad (5)$$

$$\sigma = \sqrt{\frac{1}{n} \sum_{p(x,y,z)\epsilon R(i)} (d(p(x,y,z),\alpha) - m)^2} \qquad (6)$$

where $d(p(x,y,z),\alpha)$ is the distance between point $p(x,y,z)$ and the fitting plane $\alpha$.

Since $U_{Seed}$ may have many groups of points distributed at different locations, it is denoted as $U_{Seed}$ = $\{R_1,R_2,..,R_k\}$. A point $p(x,y,z)$ in the neighborhood of group $R_i$ is included in $R_i$ for the next step of region-growing if it satisfies the homogeneity test:

$p(x,y,z)$ is either a uniform or rough surface

- $|m_i - m_j| < \lambda\times\min(\sigma_i, \sigma_j)$ , for any j $\in \overline{1,k}$,
- $| d(p(x,y,z),\alpha) - m(i)| \leq T_i$

where the thresholds $\lambda > 0$ and $T_i > 0$, which vary depending on how strict we define the background.

Figure 6 illustrates an example of the growing process where the ground can be fully retrieved by extending the neighboring regions 75 times.

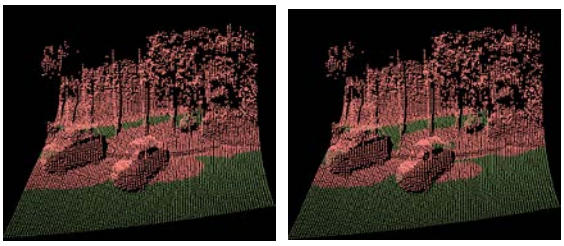

(a) (b)

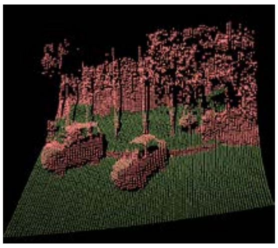

(c)

Figure 6. Region-growing for DBI: (a) the seeds for growing obtained from least-square fitting N = 0; (b) during growing progress at N = 20; and (c) the growing process stops at N = 75 when all points satisfying the homogeneity condition are included.

**Recursive search process for object marking**

After removing the background, a recursive search process is employed to find all possible objects. The strategy commonly adopted for identifying a 3-D object boundary is to keep searching from the first pixel to the end of the range image along a zigzag path and marking an object point if it exists. This strategy sometimes fails to mark objects correctly since some previously marked objects can be misclassified in the later search stage as a new object, which could require a further merging process for aliasing objects. Such extra effort is undesirable in a real-time object recognition task. Therefore, a new strategy is needed for marking the objects correctly and removing redundant objects in the search process. A solution to this is the recursive search algorithm proposed here. Instead of the method described above, the recursive method extends the search for each detected pixel until the entire object region is searched (shown in Figure 7). During recursive search, the connection to a neighboring point is broken if the distance does not satisfy the homogeneity condition, thus separating many objects from each other.

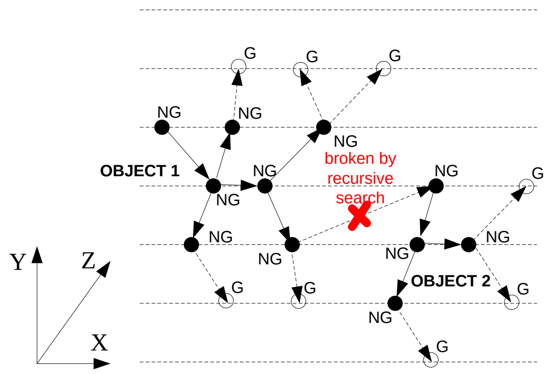


(a)

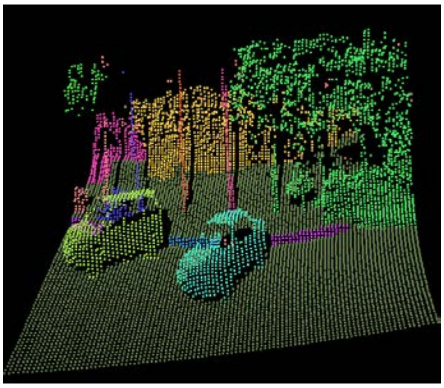

(b)

Figure 7. Path-searching strategy employed in the recursive search algorithm: (a) recursive search process (G: ground point, NG: non-ground point); and (b) example of the final result obtained using recursive search process.

The developed method employs a raster scanning pattern, which starts the search from the top-left point. A counter is used for listing all the objects in the range image; in which the counter is increased when a point of a new object is found in the search process. The recursive algorithm is designed to check all neighboring points for similarity in properties and keep continuing this extending process until all the points belonging to the same object are identified. This algorithm checks the sequence of line and column of scanning data simultaneously, thus avoiding the above-mentioned classification problem.

## EXPERIMENTAL RESULTS AND ANALYSES

The proposed method has been tested using more than 50 range images obtained by a single-point laser scanner (RIEGL LD90-3800), shown in Figure 8. To perform full-field scanning, two servo motors were used for acquisition of whole-view point clouds. One motor controlled the vertical scanning pitch, which was synchronized with RIEGL LD90-3800. The laser clock of this laser device was turned on when the vertical motor run at a constant speed for acquiring range data. After reading one vertical line, the other motor that controlled continuously the horizontal scanning pitch shifted a scanning pitch. Data were acquired simultaneously and fed to the computer during line scanning. In these examples, the detection depth ranged from 10 to 500 meters.


(a)

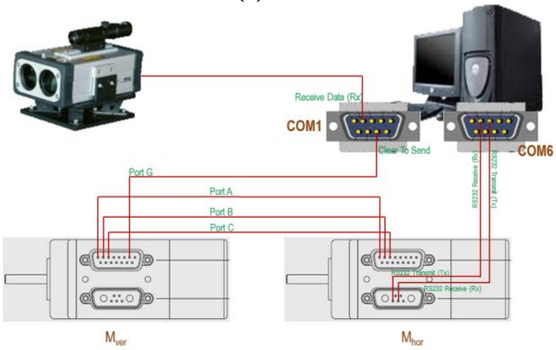


(b)

Figure 8. Laser scanner system employed in the experiment: (a) laser scanner system setup; and (b) transmittance and synchronization of obtained data by a personal computer.

Figure 9 illustrates three outdoor experimental results obtained by the developed method, with several cars serving as the detected targets for OS. While a more quantitative analysis was performed in another experiment, these examples were conducted for the feasibility test of the developed method. In such outdoor environment, the lighting condition is one of the most challenging problems encountered for achieving high S/N 3-D image acquisition. The data contain some unavoidable noises and outliers, a problem that many of the existing methods have failed to resolve. Up to now, the existing segmentation methods have mainly focused on some simple cases. Two well-known problems still prevail and are obstacles to the realization of reliable OS. One of the difficulties is failure to determine a global distance threshold that works for a large range of objects. The second problem is the low resistance to data noises distributed randomly between the foreground and background. In some scenarios with no clear cutting edge between the foreground and background, unacceptable errors in marking individual objects may result. By contrast, the proposed method can effectively resolve the issue by employing the scene ground reconstruction fitting process and by extending the largest uniform surface region. All the range images shown in Figure 9 have a resolution of 300 x 300 pixels. As seen in Figure 9(b), (d) and (f), the backgrounds have been precisely removed from the point clouds. The cars and trees are successfully marked and segmented by grouping points with similar distribution of surface indexes.

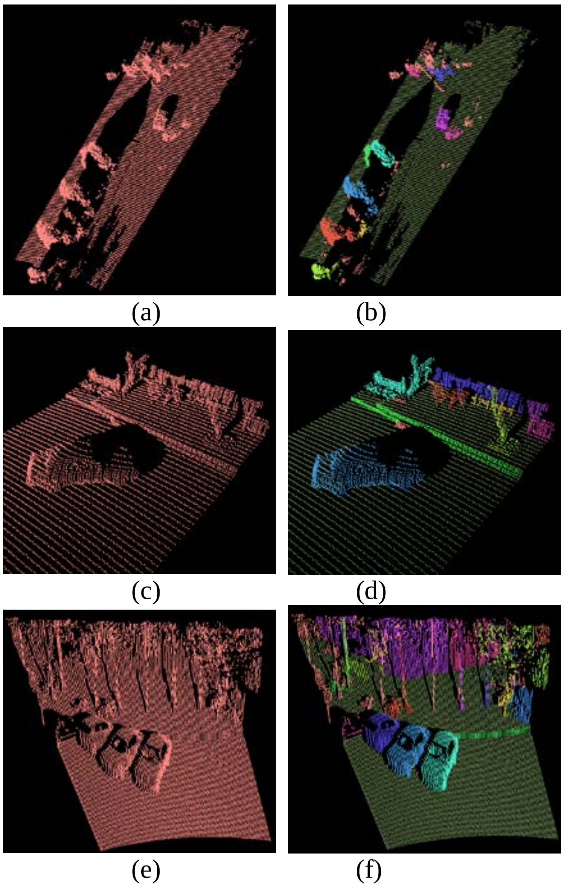


Figure 9. Segmentation examples and results: (a), (c) and (e) are 3-D range images; (b), (d) and (f) are OS results for cases (a), (c) and (e), respectively, obtained using the proposed method.

Another outdoor experiment was on automatic OS for a car in a backyard. To evaluate the performance of the proposed method against two commonly used methods (the clustering method in (Jiang et al., 1999) and the region-growing algorithm in (Evans et al., 2007), the segmentation results obtained using these three approached are compared, as shown in Figure 10. To assess the stability of each method, Gaussian noise of three levels was added to the acquired point clouds at a standard deviation of 50, 100 and 150 mm, respectively. The numbers of marked object points in the segmentation results of the car were then counted. The deviation was evaluated by calculating the difference between the number of marked object points obtained by each method and the ideal result marked by the original scene model. Comparison in terms of the deviation (percentage) in object segmentation for these three methods is shown in Figure 11. As can be seen, the OS accuracy of the developed method is controlled to be less than 10% of the total marked size of the car when Gaussian noise is increased to 150 mm while the other two methods suffer significant decrease in segmentation accuracy. The results validate the reliability of the developed method in terms of resistance to noise. Detailed of car segmentation results obtained by the proposed method are also shown in Figure 12 and Table 1.

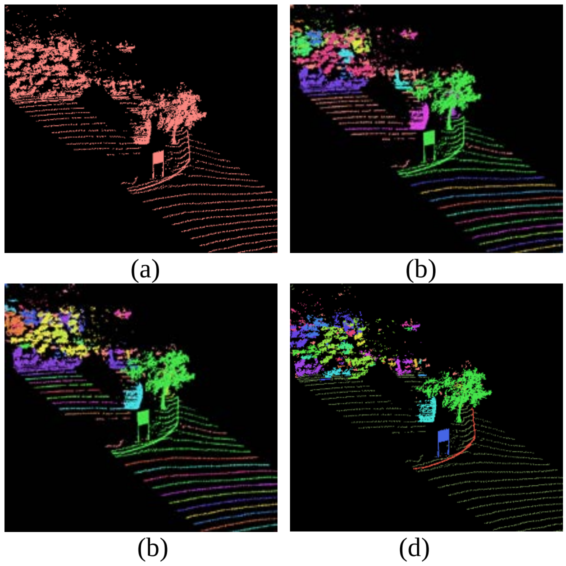


Figure 10. Segmentation example and result of a car: (a) acquired range image; segmentation by (b) the clustering method, (c) the region-growing algorithm, and (d) the proposed method.

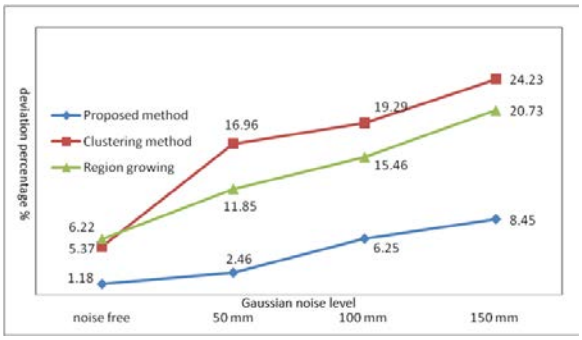


Figure 11. Comparison in terms of errors (percentage) in OS by clustering method, region-growing algorithm and the proposed method.

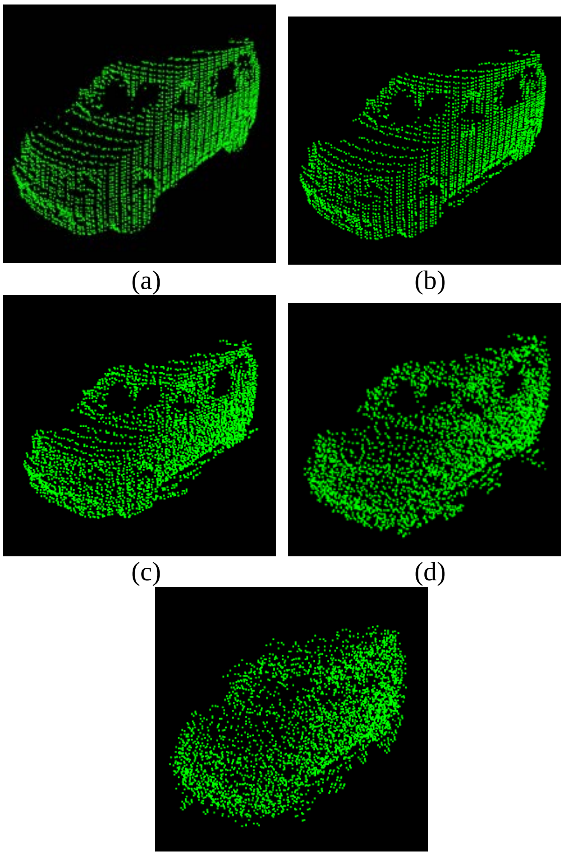

(a) (b) (c) (d) (e)

Figure 12. Segmentation results obtained by the proposed method under various conditions with three levels of Gaussian noise added. The car segmented (a) by the original model; (b) under noise-free condition; (c), (d) and (e) with Gaussian noise added at a standard deviation of 50, 100 and 150 mm, respectively.

Table 1. Segmentation results obtained by the proposed method with Gaussian noise of different levels added.

| | Segmentation results (points) | Deviation (%) |
|---|---|---|
| Correct data marked by the original object model | 3014 | - |
| noise free | 3090 | 1.18% |
| 50 mm | 3129 | 2.46% |
| 100 mm | 3245 | 6.25% |
| 150 mm | 3312 | 8.45% |

## CONCLUSIONS

An innovative object segmentation (OS) method for range images was successfully developed using surface index and scene ground-removal strategy. The proposed method has been proved feasible for complicated scenarios since its classification process only defines the surface type without requiring complicated assumption or algorithm. The developed method provides a means for detecting and mapping the trees, buildings, vehicles and other obstacles detected by laser range finders or other 3-D scanners. This research provides a feasible method in 3-D OS for further object recognition in intelligent vision systems.

## REFERENCES


Bogoslavskyi, I. and Stachniss, C., "Fast range image-based segmentation of sparse 3D laser scans for online operation," IEEE/RSJ International Conference on Intelligent Robots and Systems (IROS), Daejeon, 2016, pp. 163-169.

Chang, I. S. and Park, R. H., "Segmentation based on fusion of range and intensity images using robust trimmed methods," Pattern Recognition, Vol. 34, pp. 1951-1962, Oct. 2001.

Chang, Y. L., Li, X., "Adaptive image region-growing". Image Processing, IEEE Transactions on, Vol. 3, No. 6, pp. 868-872, 1994.

Chen, L. C., Nguyen, X. L. and Liang, C. W. "Object segmentation method using depth slicing and region-growing algorithm," International Conference on 3D Systems and Applications, Tokyo, Japan, May. 2010.

Evans, J. S. and Hudak, A. T., "A multiscale curvature algorithm for classifying discrete return LiDAR in forested environments," IEEE Transactions on Geoscience and Remote Sensing, Vol. 45, No. 4, pp. 1029-1038, 2007.

Gharavi, H,. "3-D motion estimation using range data," IEEE Trans. on Intelligent Transportation Systems, Vol. 8, No. 1, pp. 133-143, 2007.

Golovinskiy, A., Funkhouser, T., "Min-Cut-based segmentation of point clouds," IEEE Workshop on Search in 3D and Video (S3DV) at International Conference on Computer Vision, 2009.

Heisele, B. and Ritter, W., "Segmentation of range and intensity image sequences by clustering," Proceedings of the International Conference on Information Intelligence and Systems, pp. 223-225, 1999.

Holz, D. and Behnke, S. "Fast Range Image Segmentation and Smoothing Using Approximate Surface Reconstruction and Region Growing." Intelligent Autonomous Systems 12:

Volume 2 Proceedings of the 12th International Conference IAS-12, Jeju Island, Korea, 2012, pp. 61-73.

Jiang, X. and Bunke, H., “Edge detection in range images based on scan line approximation,” Comput. Vis. Image Understand., Vol. 73, No. 2, pp. 183-199, Feb. 1999.

Jiang, X., “An adaptive contour closure algorithm and its experimental evaluation,” IEEE Trans. Pattern Anal. Mach. Intell., Vol. 22, No. 11, pp. 1252-1265, Nov. 2000.

Klasing, K., Wollherr, D., and Buss, M., “A clustering method for efficient segmentation of 3D laser data,” Proceedings of the 2008 IEEE International Conference on Robotics and Automation (ICRA), Pasadena, CA, USA, pp. 4043-4048, 2008.

Koster, K. and Spann, M., “MIR: An approach to robust clustering - Application to range image segmentation,” IEEE Trans. on Pattern Analysis and Machine Intelligence, Vol. 22, No. 5, pp. 430-444, May 2000.

Lee, K. M., Meer, P. and Park, R. H. “Robust adaptive segmentation of range images,” IEEE Trans. Pattern Anal. Machine Intell., Vol. 20, pp. 200-205, Feb. 1998.

Lu, W. L., Murphy, K. P., Little, J. J., Sheffer, A. and Fu, H., “A hybrid conditional random field for estimating the underlying ground surface from airborne LiDAR data”, IEEE Transactions on Geoscience and Remote Sensing, Vol. 47, No. 8, pp. 2913-2922, 2009.

Muller, C. R., Peyrin, F., Carrillon, Y. and Oldet, C. “Automated 3D region growing algorithm based on an assessment function,” Pattern Recognition Letters, Vol. 23, pp. 137-150, 2002.

Neira, J., Tardos, J. D., Horn, J. and Schmidt, G., “Fusing range and intensity images for mobile robot localization,” IEEE Transaction on Robotics and Automation, Vol. 15, No. 1, pp. 76-84, Feb. 1999.

Pulli, K. and Pietikäinen, M., “Range image segmentation based on decomposition of surface normals,” Scandinavian Conference on Image Analysis (SCIA), Norway, 1993.

Roggero, M., “Airborne laser scanning: clustering in raw data,” in International Archives of the Photogrammetry, Remote Sensing and Spatial Information Sciences XXXIV, pp. 227-232, 2001.

Sappa, A., and Devy, M., “Fast range image segmentation by an edge detection strategy,” IEEE Int. Conf. 3-D Digital Imaging and Modeling, pp. 292-299, 2001.

Sappa, A., “Unsupervised contour closure algorithm for range image edge-based segmentation,” IEEE Transactions on Image Processing, Vol. 15, No. 2, pp. 377-384, 2006.

Silva, L., Bellon, O. R. P., and Gotardo, P. F. U., “Edge-based image segmentation using curvature sign maps from reflectance and range images,” Proceedings of International Conference on Image Processing, pp. 730-733, 2001.

Sithole, G., “Filtering of laser altimetry data using a slope adaptive filter,” in International Archives of the Photogrammetry, Remote Sensing and Spatial Information Sciences XXXIV, pp. 203-210, 2001.

Sithole, G. and Vosselman, G., “Experimental comparison of filter algorithms for bare-Earth extraction from airborne laser scanning point clouds,” ISPRS J. Photogramm. Remote Sens., Vol. 59, No. 1/2, pp. 85-101, Aug. 2004.

Stiene, S., Lingemann, K., Nuchter A. and Hertzberg, J., “Contour-based object detection in range images,” Proceedings of the Third International Symposium on 3D Data Processing, Visualization, and Transmission (3DPVT '06), pp. 168-175, 2006.

# 運用區域成長及表面分類之創新三維影像分割技術

陳亮嘉
國立台灣大學機械工程學系

陳亮嘉 梁景文 阮春祿
國立台北科技大學自動化所

林世聰
國立台北科技大學光電工程所

## 摘要

本文提出了一種運用表面特徵之創新三維影像分割物件技術。在自動化光學檢測運用領域，為了解決雷射掃描儀掃描三維影像的數位背景識別（DBI）問題，此方法提出了一種基於表面法向量分佈的創新判別標準與方法。三維影像依據該判別標準被分類為三種類型的表面，作為識別背景點評估的初始步驟，本方法以遞歸搜索程序將該判別標準導入區域成長方法，建立具備適用於同特徵表面區域的區域成長演算法，經由評估表面法向量的分佈來識別與正確分類三種表面類型。同時，為了準確地偵測個別物件的精確邊界位置，提出區域成長的方法。為驗證本方法的實際能力，使用雷射三維

掃描儀對多種室外充斥大量雜訊狀況場景進行三維影像之取像與處理多個實驗，在150 mm標準差的高斯分佈雜訊的距離影像，本法可以對三維物體進行自動化物件精確分割，執行正確率可高於大於90%，初步證明所提出的方法可有效分割複雜物體的三維影像。